Tetranuclear heteroleptic mercury(II) complexes of the composition $[Hg_4(S_2CNPr_2)_6(NO_3)_2]$ and $[Hg_4(S_2CNPr_2)_4Cl_4]$: structural organization, principles of construction of supramolecular polymeric chains, and thermal behavior*

O. V. Loseva,[a] T. A. Rodina,[b] A. V. Ivanov,[a]★ A. I. Smolentsev,[c,d] and O. N. Antzutkin[e,f]

[a]*Institute of Geology and Nature Management, Far Eastern Branch of the Russian Academy of Sciences,*
1 Relochnyi per., 675000 Blagoveshchensk, Russian Federation.
Fax: +7 (416 2) 22 5325. E-mail: alexander.v.ivanov@chemist.com
[b]*Amur State University,*
21 Ignatievskoe shosse, 675027 Blagoveshchensk, Russian Federation
[c]*Nikolaev Institute of Inorganic Chemistry, Siberian Branch of the Russian Academy of Sciences,*
3 prosp. Akad. Lavrentieva, 630090 Novosibirsk, Russian Federation
[d]*Novosibirsk State University,*
1 ul. Pirogova, 630090 Novosibirsk, Russian Federation
[e]*Luleå University of Technology, SE-971 87 Luleå, Sweden*
[f]*The University of Warwick, Coventry CV4 7AL, United Kingdom*

New heteroleptic mercury(II) complexes $[Hg_4(S_2CNPr_2)_6(NO_3)_2]$ (**1**) and $[Hg_4(S_2CNPr_2)_4Cl_4]$ (**2**) were synthesized and characterized by single-crystal X-ray diffraction and ^{13}C and ^{15}N MAS NMR spectroscopy. In these complexes, the metal atoms are linked in pairs by bridging dipropyldithiocarbamate ligands (Pr_2Dtc) to form tetranuclear cations and molecules. The further structural organization of compound **1** to the polymeric chains $[Hg_4(S_2CNPr_2)_6(NO_3)_2]_n$ occurs due to the linking of $[Hg_4(S_2CNPr_2)_6]^{2+}$ cations by pairs of bridging nitrate groups. The formation of the supramolecular polymeric structure of **2** is determined by pairwise secondary Hg···Cl bonds between the cyclic $[Hg_4(S_2CNPr_2)_4Cl_4]$ molecules, in which the central eight-membered metallocycle $[Hg_4S_4]$ adopts a distorted chair conformation. The thermal behavior of compounds **1** and **2** was studied by simultaneous thermal analysis.

Key words: tetranuclear mercury(II) complexes, polymeric compounds, dialkyldithiocarbamates, supramolecular self-organization, secondary interactions, thermal behavior.

Mononuclear mercury(II) complexes with coordination number (CN) 4 can have both square-planar and distorted tetrahedral structures, which correspond to the sp^2d- and sp^3-hybrid state of the central mercury atom. However, the interaction with nearest neighbors can be accompanied by an increase in CN (from 4 to 5 or 6), thereby completing the coordination polyhedron of mercury to a distorted tetragonal pyramid, a trigonal bipyramid, or a distorted octahedron (sp^3d- and sp^3d^2-hybrid state).[1] According to the Lewis theory, the mercury(II) cation is a soft acid. Due to this fact, along with their chalcophilic properties, these cations are highly prone to complexation with sulfur-containing ligands acting as soft bases. Therefore, chelate S,S'-coordinating dialkyl- and alkylenedithiocarbamate ligands efficiently coordinate mercury(II) to form complexes having low solubility products (SP $1.91 \cdot 10^{-39}$—$5.50 \cdot 10^{-51}$). This fact is of great interest for the detection and detoxification of mercury ion poisoning.[2—5] It should be noted that mercury(II) dithiocarbamate complexes are technological precursors in one-step thermochemical processes for the fabrication of thin-film and nanocrystalline mercury sulfides. Due to a narrow band gap, the latter are promising semiconductor materials for the design of ultrasonic sensors, photoelectric converters, infrared detectors, catalysts, *etc.*[6—9] Another practically important property of mercury(II) dithiocarbamates is their ability to efficiently concentrate gold(III) from acidic (2*M* HCl) solutions, forming double ionic-polymer Hg^{II}—Au^{III} complexes as individual forms of chemisorption binding of gold.[10—12]

Dithiocarbamate ligands can perform different structural functions (monodentate, bidentate terminal, bridging,
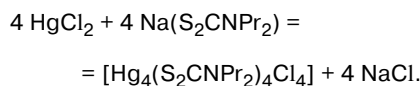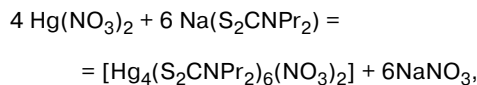
or mixed), which makes them convenient and versatile synthons for the targeted synthesis of homo- and hetero-leptic mercury(II) complexes with intricate supramolecular architectures involving secondary Hg⋯S bonds, C—H⋯S hydrogen bonds, and C—H⋯π interactions.[13—21] The anions utilized in the synthesis of metal salts also play an important role in the formation of the inner coordination sphere of the complexes. Being nucleophilic species, they are capable of hydrogen bonding, can be involved in electrostatic interactions, and are able to control the self-assembly of complexes, by influencing their composition, structure, and properties.

In the present work, we synthesized and structurally characterized new heteroleptic tetranuclear mercury(II) complexes $[Hg_4(S_2CNPr_2)_6(NO_3)_2]_n$ (**1**) and $[Hg_4(S_2CN-Pr_2)_4Cl_4]_n$ (**2**), which form polymeric chains at the supra-molecular level. The structural organization and thermal behavior of compounds **1** and **2** were studied by X-ray diff-raction, ^{13}C and ^{15}N magic-angle spinning (MAS) NMR spectroscopy, and simultaneous thermal analysis (STA).

Results and Discussion

Compounds **1** and **2** were prepared by precipitation of Hg^{2+} ions with sodium dipropyldithiocarbamate, taken in a stoichiometric ratio, from an aqueous phase according to the following reactions:

$$4\, Hg(NO_3)_2 + 6\, Na(S_2CNPr_2) =$$
$$= [Hg_4(S_2CNPr_2)_6(NO_3)_2] + 6NaNO_3,$$

$$4\, HgCl_2 + 4\, Na(S_2CNPr_2) =$$
$$= [Hg_4(S_2CNPr_2)_4Cl_4] + 4\, NaCl.$$

The unit cells of tetranuclear compounds **1** and **2** contain two and one formula units, $[Hg_4(S_2CNPr_2)_6(NO_3)_2]$ and $[Hg_4(S_2CNPr_2)_4Cl_4]$, respectively (Figs 1 and 2). These complexes include dipropyldithiocarbamate (Pr_2Dtc) ligands, playing the same μ_2-bridging structural function. Therefore, before discussing the structural or-ganization of **1** and **2**, let us consider the general charac-teristics of Pr_2Dtc ligands.

The significantly shorter formally single N—C bonds in $=NC(S)S$ groups of compounds **1** and **2** (1.29—1.36 Å and 1.316, 1.321 Å, respectively) compared to those in the peripheral part of the ligands (N—CH$_2$, 1.44—1.51 and 1.465—1.477 Å, respectively) are indicative of a consider-able contribution of the double bonding character due to the mesomeric effect of dithiocarbamate groups. This is also the cause of the efficient averaging of the C—S bond lengths in Pr_2Dtc ligands (1.71—1.76 Å); in each ligand, the observed difference in the bond lengths is fairly small (0—0.04 Å, see Tables 1 and 2). Besides, the mutual ar-rangement of atoms in the structural moieties C_2NCS_2
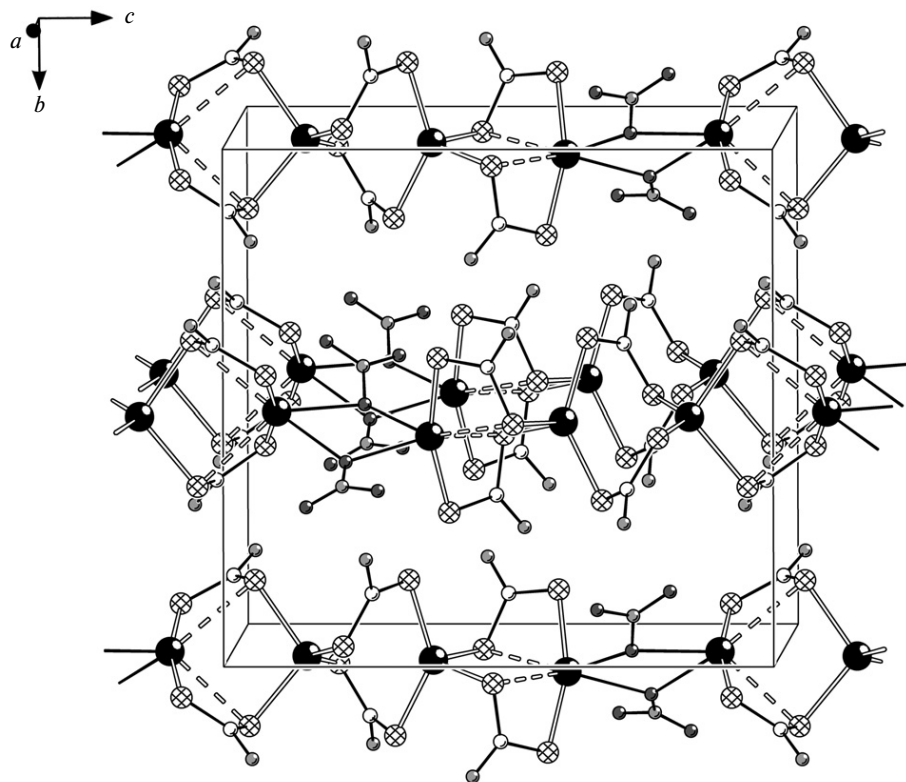
Fig. 1. Packing of structural units of complex **1** projected onto the *bc* plane. Alkyl substituents in Pr_2Dtc ligands are not shown.
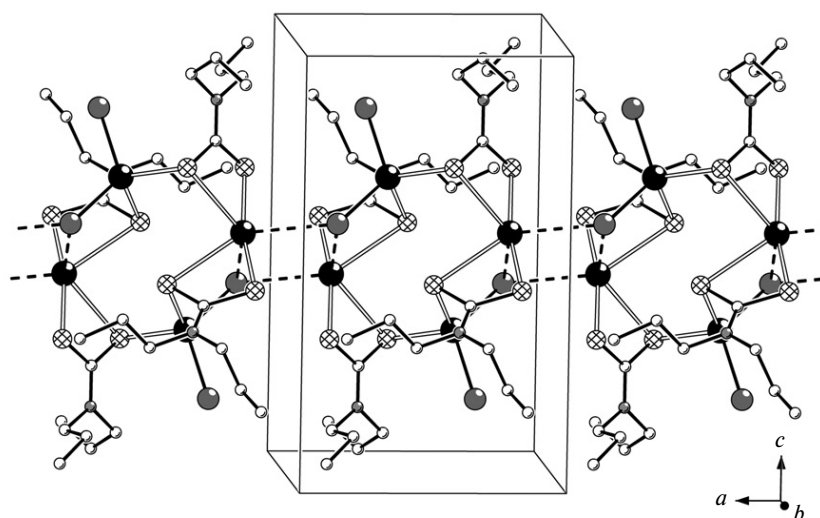
Fig. 2. Unit cell of complex **2** projected onto the *ac* plane. Intra- and intermolecular secondary Hg···Cl bonds are indicated by dashed lines.

deviates little from coplanarity; the deviations of the SCNC torsion angles from 0° or 180° are 0.5—13.2° and 2.4—5.4° for compounds **1** and **2**, respectively (Tables 3 and 4).

In complex **1**, all alike structural subunits (mercury atoms, dithiocarbamate ligands, and nitrate groups) are structurally nonequivalent. Adjacent mercury atoms are

Table 1. Selected bond lengths and interatomic distances (*d*) in compound **1**, $[Hg_4(S_2CNPr_2)_6(NO_3)_2]$

Bond	*d*/Å	Bond	*d*/Å
Hg(1)—S(1)	2.402(5)	S(3)—C(8)	1.75(2)
Hg(1)···S(2)	3.074(5)	S(4)—C(8)	1.74(2)
Hg(1)—S(3)	2.402(5)	S(5)—C(15)	1.72(2)
Hg(1)···S(4)	3.062(5)	S(6)—C(15)	1.71(2)
Hg(2)—S(2)	2.648(4)	S(7)—C(22)	1.73(2)
Hg(2)—S(4)	2.601(5)	S(8)—C(22)	1.73(2)
Hg(2)—S(5)	2.469(5)	S(9)—C(29)	1.74(3)
Hg(2)—S(7)	2.496(5)	S(10)—C(29)	1.76(2)
Hg(3)—S(6)	2.502(5)	S(11)—C(36)	1.75(2)
Hg(3)—S(8)	2.489(5)	S(12)—C(36)	1.72(2)
Hg(3)—S(9)	2.598(5)	N(1)—C(1)	1.29(3)
Hg(3)—S(11)	2.565(5)	N(2)—C(8)	1.32(3)
Hg(4)···S(9)	3.133(5)	N(3)—C(15)	1.34(3)
Hg(4)—S(10)	2.388(5)	N(4)—C(22)	1.36(2)
Hg(4)···S(11)	3.074(5)	N(5)—C(29)	1.30(3)
Hg(4)—S(12)	2.401(5)	N(6)—C(36)	1.35(3)
Hg(1)—O(1)	2.657(15)	O(1)—N(7)	1.24(2)
Hg(1)—O(4)	2.522(14)	O(2)—N(7)	1.25(2)
Hg(4)—O(1)[#a]	2.645(16)	O(3)—N(7)	1.28(2)
Hg(4)—O(4)[#a]	2.713(14)	O(4)—N(8)	1.22(2)
S(1)—C(1)	1.72(2)	O(5)—N(8)	1.20(2)
S(2)—C(1)	1.76(3)	O(6)—N(8)	1.21(2)

Note. Symmetry code: [#a] *x, y*, 1 + *z*.

Table 2. Selected bond lengths and interatomic distances (*d*) in compound **2**, $[Hg_4(S_2CNPr_2)_4Cl_4]$

Bond	*d*/Å	Bond	*d*/Å
Hg(1)—S(1)	2.3744(11)	S(1)—C(1)	1.735(4)
Hg(1)—S(2)	3.0050(11)	S(2)—C(1)	1.735(4)
Hg(1)—S(3)	2.3673(11)	S(3)—C(8)	1.732(5)
Hg(1)—S(4)	3.0474(12)	S(4)—C(8)	1.741(4)
Hg(1)···Cl(1)	3.1388(12)	N(1)—C(1)	1.316(5)
Hg(1)···Cl(1)[#b]	3.1656(11)	N(1)—C(2)	1.465(6)
Hg(2)—S(2)	2.5636(11)	N(1)—C(5)	1.477(5)
Hg(2)—S(4)[#a]	2.5583(11)	N(2)—C(8)	1.321(5)
Hg(2)—Cl(1)	2.4905(11)	N(2)—C(9)	1.469(6)
Hg(2)—Cl(2)	2.4464(13)	N(2)—C(12)	1.470(7)

Note. Symmetry codes: [#a] 1 −*x*, 1 − *y*, 1 − *z*; [#b] − *x*, 1 − *y*, 1 − *z*.

linked in pairs by μ_2-bridging Pr$_2$Dtc ligands to form the nearly linear tetranuclear cation $[Hg_4(S_2CNPr_2)_6]^{2+}$; the Hg(1)Hg(2)Hg(3) and Hg(2)Hg(3)Hg(4) angles are 179.04° and 173.36°, respectively; the interatomic Hg—Hg distances are as follows: Hg(1)—Hg(2), 3.800 Å; Hg(2)—Hg(3), 3.558 Å; Hg(3)—Hg(4), 3.870 Å (see Fig. 2)*. The bidentate bridging ligands that link the Hg(2) and Hg(3) atoms form four Hg—S bonds, with the lengths varying in the narrow range of 2.469—2.502 Å. This results in the formation of the extended eight-membered metallocycle

---

* Previously, the structures of complex cations containing an odd number of mercury(II) atoms (tri- and pentanuclear cations), which include diethyldithiocarbamate ligands, $[Hg_3(S_2CNEt_2)_4]^{2+}$ and $[Hg_5(S_2CNEt_2)_8]^{2+}$, have been dscribed.[22] The hexanuclear molecular complex with the diethylmonothiocarbamate ligand, $[Hg_6\{S(O)CNEt_2\}_{12}]$, was also synthesized.[23]

Table 3. Selected bond angles (ω) and torsion angles (φ) in compound **1**, $[Hg_4(S_2CNPr_2)_6(NO_3)_2]$

Parameter	Value	Parameter	Value
Bond angle	ω/deg	Bond angle	ω/deg
S(1)—Hg(1)—S(3)	161.45(17)	S(7)—C(22)—N(4)	118.4(17)
S(2)—Hg(2)—S(4)	106.60(15)	S(8)—C(22)—N(4)	117.5(16)
S(2)—Hg(2)—S(5)	106.48(18)	S(9)—C(29)—S(10)	120.9(14)
S(2)—Hg(2)—S(7)	94.65(18)	S(9)—C(29)—N(5)	122.1(19)
S(4)—Hg(2)—S(5)	101.93(18)	S(10)—C(29)—N(5)	117.0(19)
S(4)—Hg(2)—S(7)	105.91(17)	S(11)—C(36)—S(12)	119.6(12)
S(5)—Hg(2)—S(7)	138.29(18)	S(11)—C(36)—N(6)	120.0(16)
S(6)—Hg(3)—S(8)	134.79(17)	S(12)—C(36)—N(6)	120.2(16)
S(6)—Hg(3)—S(9)	94.71(18)	C(1)—N(1)—C(2)	121.4(19)
S(6)—Hg(3)—S(11)	113.28(17)	C(1)—N(1)—C(5)	125.2(19)
S(8)—Hg(3)—S(9)	109.65(18)	C(8)—N(2)—C(9)	121.0(19)
S(8)—Hg(3)—S(11)	96.2(2)	C(8)—N(2)—C(12)	119.9(18)
S(9)—Hg(3)—S(11)	106.10(15)	C(15)—N(3)—C(16)	123.7(19)
S(10)—Hg(4)—S(12)	164.63(17)	C(15)—N(3)—C(19)	122.3(17)
O(1)—Hg(1)—O(4)	63.8(4)	C(22)—N(4)—C(23)	121.5(19)
O(1)[#a]—Hg(4)—O(4)[#a]	61.5(4)	C(22)—N(4)—C(26)	123.8(18)
Hg(1)—O(1)—Hg(4)[#b]	114.0(6)	C(29)—N(5)—C(30)	123(2)
Hg(1)—O(4)—Hg(4)[#b]	116.2(5)	C(29)—N(5)—C(33)	124(2)
S(1)—C(1)—S(2)	119.3(16)	C(36)—N(6)—C(37)	122.9(18)
S(1)—C(1)—N(1)	123(2)	C(36)—N(6)—C(40)	124.1(19)
S(2)—C(1)—N(1)	118.1(18)	N(7)—O(1)—Hg(4)	101.3(12)
S(3)—C(8)—S(4)	117.7(12)	N(7)—O(1)—Hg(1)	128.7(13)
S(3)—C(8)—N(2)	119.9(17)	O(1)—N(7)—O(2)	120.5(18)
S(4)—C(8)—N(2)	122.4(17)	O(1)—N(7)—O(3)	116.7(18)
S(5)—C(15)—S(6)	124.3(13)	O(2)—N(7)—O(3)	122.5(18)
S(5)—C(15)—N(3)	116.8(17)	O(5)—N(8)—O(6)	121(2)
S(6)—C(15)—N(3)	118.9(17)	O(5)—N(8)—O(4)	122(2)
S(7)—C(22)—S(8)	124.0(11)	O(6)—N(8)—O(4)	116.4(19)
Torsion angle	φ/deg	Torsion angle	φ/deg
S(1)—C(1)—N(1)—C(2)	4(3)	S(7)—C(22)—N(4)—C(23)	−11(3)
S(1)—C(1)—N(1)—C(5)	−179.1(16)	S(7)—C(22)—N(4)—C(26)	174.3(15)
S(2)—C(1)—N(1)—C(2)	−178.9(15)	S(8)—C(22)—N(4)—C(23)	171.1(15)
S(2)—C(1)—N(1)—C(5)	−2(3)	S(8)—C(22)—N(4)—C(26)	−3(3)
S(3)—C(8)—N(2)—C(9)	2(3)	S(9)—C(29)—N(5)—C(30)	−1(3)
S(3)—C(8)—N(2)—C(12)	175.3(14)	S(9)—C(29)—N(5)—C(33)	−178.8(16)
S(4)—C(8)—N(2)—C(9)	177.1(15)	S(10)—C(29)—N(5)—C(30)	178.4(17)
S(4)—C(8)—N(2)—C(12)	−4(3)	S(10)—C(29)—N(5)—C(33)	1(3)
S(5)—C(15)—N(3)—C(16)	−11(3)	S(11)—C(36)—N(6)—C(37)	3(3)
S(5)—C(15)—N(3)—C(19)	165.9(14)	S(11)—C(36)—N(6)—C(40)	−168.6(16)
S(6)—C(15)—N(3)—C(16)	170.1(15)	S(12)—C(36)—N(6)—C(37)	178.3(15)
S(6)—C(15)—N(3)—C(19)	−13(3)	S(12)—C(36)—N(6)—C(40)	6(3)

Note. Symmetry codes: [#a] x, y, $1 + z$; [#b] x, y, $z − 1$.

$[Hg_2S_4C_2]$ stabilized in a saddle conformation*.[25] Each mercury atom (the coordination number (CN) 4) has a distorted tetrahedral environment formed by sulfur atoms of four Pr_2Dtc ligands; the SHgS angles are in the range of 94.65—113.28°, except for the S(5)Hg(2)S(7) (138.29°) and S(6)Hg(3)S(8) (134.79°) angles (Fig. 3).

---

* Previously, we have described such conformations for metallocycles of the composition $[Cd_2S_4P_2]$ in polymeric cadmium(II) dialkyldithiophosphates.[24]

Four other Pr_2Dtc ligands involved in the binding of mercury atoms in pairs (Hg(1), Hg(2) and Hg(3), Hg(4)) are characterized by tridentate bridging coordination. Each of these ligands is coordinated in a S,S′-anisobidentate fashion to terminal mercury atoms, Hg(1) or Hg(4), to form four-membered metallocycles $[HgS_2C]$. In these metallocycles, the Hg—S bonds are significantly different. For the first group of bonds (2.388—2.402 Å), the lengths are consistent with the sum of the covalent radii of the mercury and sulfur atoms (2.34 Å),[26] whereas the bonds

Table 4. Selected bond angles (ω) and torsion angles (φ) in compound **2**, [Hg$_4$(S$_2$CNPr$_2$)$_4$Cl$_4$]

Parameter	Value	Parameter	Value
Bond angle	ω/deg	Bond angle	ω/deg
S(1)—Hg(1)—S(2)	66.67(3)	S(4)—C(8)—N(2)	121.4(3)
S(1)—Hg(1)—S(3)	165.41(4)	C(1)—N(1)—C(2)	123.2(4)
S(1)—Hg(1)—S(4)	112.73(3)	C(1)—N(1)—C(5)	121.5(4)
S(2)—Hg(1)—S(3)	125.76(4)	C(2)—N(1)—C(5)	115.3(3)
S(2)—Hg(1)—S(4)	80.33(3)	C(8)—N(2)—C(9)	122.1(4)
S(3)—Hg(1)—S(4)	66.20(3)	C(8)—N(2)—C(12)	123.0(5)
Hg(1)—S(1)—C(1)	96.12(14)	C(9)—N(2)—C(12)	114.9(5)
Hg(1)—S(2)—C(1)	76.04(15)	Cl(1)—Hg(2)—Cl(2)	119.79(5)
Hg(1)—S(3)—C(8)	96.74(15)	S(4)$^{\#a}$—Hg(2)—S(2)	106.51(4)
Hg(1)—S(4)—C(8)	74.96(15)	Hg(1)—S(2)—Hg(2)	89.55(3)
S(1)—C(1)—S(2)	119.8(2)	Hg(1)—S(4)—Hg(2)$^{\#a}$	100.89(4)
S(1)—C(1)—N(1)	119.3(3)	Cl(1)—Hg(2)—S(2)	100.12(4)
S(2)—C(1)—N(1)	120.8(3)	Cl(1)—Hg(2)—S(4)$^{\#a}$	111.53(4)
S(3)—C(8)—S(4)	120.3(2)	Cl(2)—Hg(2)—S(2)	110.30(5)
S(3)—C(8)—N(2)	118.3(3)	Cl(2)—Hg(2)—S(4)$^{\#a}$	107.71(4)
Torsion angle	φ/deg	Torsion angle	φ/deg
Hg(1)—S(1)—S(2)—C(1)	−166.4(3)	S(2)—C(1)—N(1)—C(2)	−175.0(3)
Hg(1)—S(3)—S(4)—C(8)	164.1(3)	S(2)—C(1)—N(1)—C(5)	5.4(6)
S(1)—Hg(1)—C(1)—S(2)	−168.5(2)	S(3)—C(8)—N(2)—C(9)	−2.4(6)
S(3)—Hg(1)—C(8)—S(4)	166.6(3)	S(3)—C(8)—N(2)—C(12)	176.2(4)
S(1)—C(1)—N(1)—C(2)	2.4(6)	S(4)—C(8)—N(2)—C(9)	176.5(4)
S(1)—C(1)—N(1)—C(5)	−177.1(3)	S(4)—C(8)—N(2)—C(12)	−4.9(7)

Note. Symmetry code: $^{\#a}1 - x, 1 - y, 1 - z$.
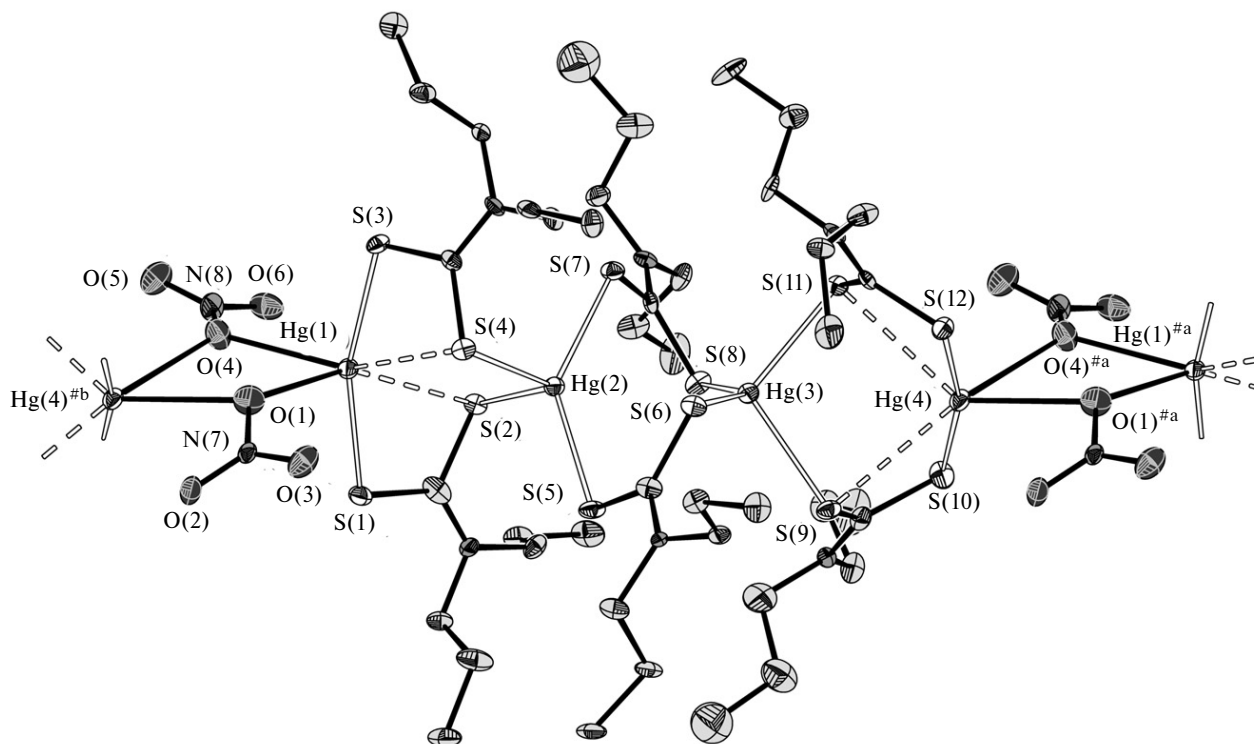
Fig. 3. Fragment of the polymeric chain [Hg$_4$(S$_2$CNPr$_2$)$_6$(NO$_3$)$_2$]$_n$ with thermal ellipsoids drawn at the 30% probability level. Hydrogen atoms are not shown. The weakest Hg···S bonds are indicated by dashed lines.

in the second group (3.062—3.133 Å) are substantially weakened and their lengths are closer to the sum of the van der Waals radii of the atoms under consideration (3.50 Å),[26] which indicates that the latter bonds are similar to secondary Hg···S bonds*. These weakly bound sulfur atoms are involved in the coordination to the adjacent mercury atoms, Hg(2) or Hg(3), and belong to the third group of covalent Hg—S bonds (2.565—2.648 Å). The binding of the mercury atoms in pairs is accompanied by the formation of tricyclic systems $[Hg_2S_4C_2]$. When excluding the weakest Hg···S bonds, the conformation of the latter systems can be approximately described as a distorted saddle.

The tetranuclear cations are linked together to the polymeric chain $[Hg_4(S_2CNPr_2)_6(NO_3)_2]_n$ by two non-equivalent μ_2-bridging nitrate groups. In each group, one oxygen atom, O(1) or O(4), is asymmetrically coordinated to the terminal mercury atoms, Hg(1) and Hg(4)[#b], of the adjacent cationic moieties (see Fig. 3). (The nonlinear structure of the chain is evidenced by the Hg(3)Hg(4)-Hg(1)[#a] and Hg(4)[#b]Hg(1)Hg(2) angles equal to 158.95° and 164.77°, respectively). Therefore, the inner coordination sphere of the mercury atoms Hg(1)/Hg(4) is completed to distorted octahedra $[HgS_4O_2]$ (CN 6) due to additional

---

* The concept of secondary bonds was proposed by Alcock.[27]

coordination. The equatorial planes include oxygen atoms and the sulfur atoms S(2), S(4)/S(9), S(11) bound by secondary bonds. The axial positions are occupied by the S(1), S(3)/S(10), S(12) atoms. The axial S(1)Hg(1)-S(3)/S(10)Hg(2)S(12) angles are 161.45°/164.63°. In the equatorial plane of the octahedra, the diagonal SHgO angles also significantly deviate from 180° in opposite directions, which attests to substantial tetrahedral distortions (154.27°, 140.28°/149.25°, and 135.27°).

The nitrate groups have a trigonal-planar structure due to the sp^2-hybrid state of the nitrogen atoms. The N—O bond lengths (1.20—1.28 Å) and the ONO bond angles (101.3—128.7°) are typical of nitrate ions.[1] Each nitrate group involved in the binding of the tetranuclear cations forms two O—Hg bonds, one of which is somewhat shorter than another one (Hg(4)—O(1), 2.645 Å; Hg(1)—O(1), 2.657 Å; Hg(1)—O(4), 2.522 Å; Hg(4)—O(4), 2.713 Å). These bond lengths are intermediate between the sums of the covalent and van der Waals radii of the mercury and oxygen atoms (1.98 and 3.22 Å, respectively[22]), due to which they can be considered as weak covalent bonds.

The structure of tetranuclear complex **2** includes pairs of nonequivalent mercury atoms, chlorine atoms, and Pr_2Dtc ligands. For convenience of consideration, two molecular units, $[Hg(S_2CNPr_2)_2]$ and $HgCl_2$, can be formally distinguished in structure **2**, (Fig. 4). In the for-
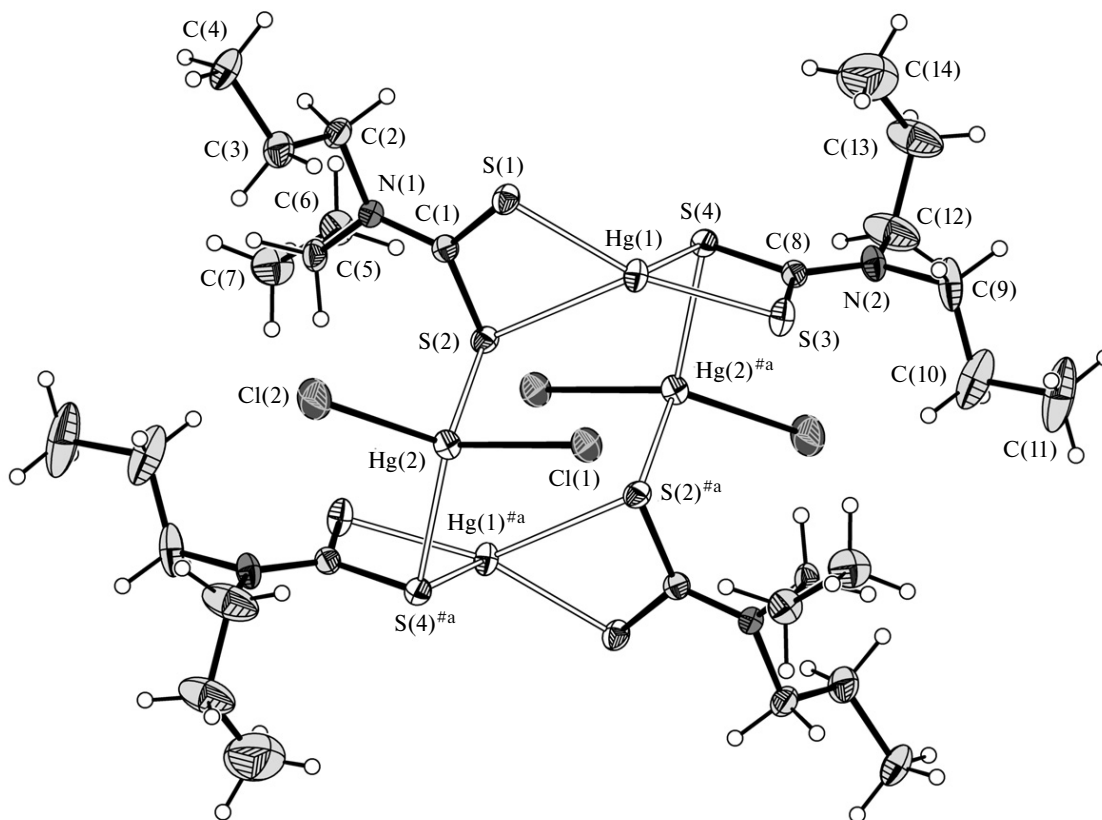

Fig. 4. Tetranuclear cyclic molecule $[Hg_4(S_2CNPr_2)_4Cl_4]$ with thermal ellipsoids drawn at the 50% probability level.

mer units, the Hg(1) atom is coordinated in a S,S′-aniso-bidentate fashion by two nonequivalent dithiocarbamate ligands, with essentially different Hg—S bond lengths (2.3744, 3.0050 Å [S(2)] and 2.3673, 3.0474 Å [S(4)]; see Table 2). The coordination results in the formation of two four-membered metallocycles [HgS$_2$C] that are linked together by a mercury atom to the bicyclic system [CS$_2$HgS$_2$C]. However, the sulfur atoms S(2) and S(4) additionally form the stronger Hg(2)—S bonds (2.5636 and 2.5583 Å) with the structural units HgCl$_2$, with the result that the central mercury atom adopts a distorted tetrahedral environment [Cl$_2$S$_2$]; the L—Hg(2)—L angles vary in the range of 100.12—119.79° (see Fig. 4, Table 4). The involvement of these bonds in the connection of the structural units [Hg(S$_2$CNPr$_2$)$_2$] and HgCl$_2$ leads to the formation of cyclic tetranuclear molecules [Hg$_4$(S$_2$CNPr$_2$)$_4$Cl$_4$] (2), which are additionally structurally stabilized by two intra-molecular secondary Hg(1)···Cl(1) bonds (3.1388 Å; see Fig. 2). For comparison, the Hg(2)—Cl(1) and Hg(2)—Cl(2) bond lengths are 2.4905 and 2.4464 Å, respectively, the sum of the van der Waals and covalent radii of these atoms are 3.45 and 2.34 Å, respectively.[26] In molecule 2, the conformation of the central eight-membered ring [Hg$_4$S$_4$] composed of alternating mercury and sulfur atoms can be approximately described as a distorted chair,[24] the geometry of which is characterized by the presence of a center of symmetry.[25] Pairwise intermolecular secondary Hg(1)···Cl(1)$^{\#b}$ interactions (3.1656 Å) play a key role in the supramolecular self-organization of tetranuclear molecules to the polymeric chain [Hg$_4$(S$_2$CNPr$_2$)$_4$Cl$_4$]$_n$ (see Fig. 2, Table 2).

The MAS NMR spectra of complex 2 show pairs of equally intense ^{13}C and ^{15}N resonance lines of dithiocarbamate groups, which attest to an individual nature of the compound and is in complete agreement with the presence of two nonequivalent Pr$_2$Dtc ligands in its structure. (In the ^{13}C NMR spectrum, alkyl substituents of the ligands appear as the corresponding numbers of resonance signals of =NCH$_2$—, —CH$_2$—, and —CH$_3$ groups; see the Experimental). The chemical shifts δ(^{13}C) (198.8, 197.7 ppm) and δ(^{15}N) (152.5, 152.0 ppm) are in the region characteristic of =NC(S)S— groups with a bridging structural function.[15,28] According to the ^{13}C and ^{15}N MAS NMR data, polycrystalline samples, which were produced in the synthesis of complex 1 along with the tetranuclear complex [Hg$_4$(S$_2$CNPr$_2$)$_6$(NO$_3$)$_2$], include the binuclear compound of the composition [Hg$_2$(S$_2$CNPr$_2$)$_4$] (see the Experimental). The latter fact leads to the mutual overlap of the resonance ^{13}C NMR signals of the =NCH$_2$—, —CH$_2$—, and —CH$_3$ groups of alkyl substituents. Hence, let us consider the MAS NMR data only for =NC(S)S— groups, which are most informative from the structural point of view. In the experimental ^{13}C and ^{15}N NMR spectra, dithiocarbamate groups of complex 1 appear as five and four resonance signals, respectively (in each case, one signal is characterized by a two- or three-fold intensity, respectively), which is consistent with the X-ray diffraction data demonstrating the presence of six nonequivalent Pr$_2$Dtc ligands in structure 1. The chemical shifts δ(^{13}C) and δ(^{15}N) of the latter are indicative of their bridging function.[15,28] The low-intensity signal at δ 336.3 is assigned to nitrate groups.

The thermal behavior of the complexes was studied by simultaneous thermal analysis (STA) under an argon atmosphere by simultaneously recording thermogravimetric (TG) and differential scanning calorimetry (DSC) curves. Compounds 1 and 2 are thermally stable up to ~115 and ~150 °C, respectively Before the onset of weight loss, the DSC curve of complex 1 exhibits a low-intensity endothermic effect at 101.1 °C, which was assigned to the melt-
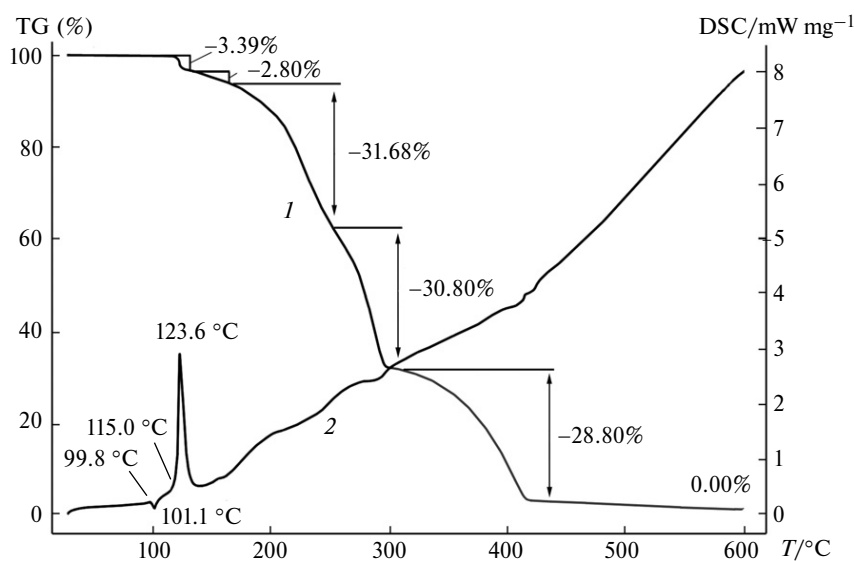

Fig. 5. TG (*1*) and DSC (*2*) curves of complex 1.

ing of **1**. The extrapolated melting point is 99.8 °C (Fig. 5, curve *2*). In an independent experiment in a glass capillary, the melting of the sample was observed in the temperature range of 100—102 °C.

The TG curve has several inflection points character-izing thermal decomposition stages of **1** (see Fig. 5, curve *1*). The initial thermolysis stage (~115—165 °C) includes two weight loss steps (3.39 and 2.80%, in total 6.19%), which is in agreement with the calculated weight of two nitrate groups (6.25%). Thermal transformations at relatively low temperatures due to the dissociation of NO_3 groups are typical of nitrate complexes.[29] This process is reflected in the DSC curve as an intense exothermic effect with an extreme at 123.6 °C (the extrapolated temperature is 115.0 °C). The main weight loss of 62.48% is observed in the next steeply sloped region of the TG curve (~165—310 °C) due to the thermolysis of the dithiocarbamate part of the complex giving HgS as the major final product*. However, the experimental value is 15.63% higher than the calculated weight loss (46.85%) in this process. The char-acteristic final step in the TG curve (~310—435 °C) asso-ciated with the sublimation of HgS (28.80%), on the contrary, reflects the underestimated weight loss compared to the calculated value (46.90%). However, the missing weight in this step of the TG curve is comparable to the excess weight in the previous stage. Therefore, the sublimation of the resulting HgS evidently starts well below 310 °C, thereby overlapping with the thermal decomposition of

the dithiocarbamate part of the complex. This distinguish-ing feature of HgS sublimation during the thermolysis of mercury(II) dithiocarbamates was observed in our previous studies.[11,12,21] The final gently sloping region of the TG curve (435—600 °C) is associated with the gradual desorp-tion of low-volatile decomposition products (2.53%).

The TG curve of complex **2** shows three weakly pronounced weight loss steps (Fig. 6, curve *1*). The first step (~150—263 °C) is associated with the thermolysis of the cyclic tetranuclear molecules $[Hg_4(S_2CNPr_2)_4Cl_4]$ accompanied by the release of $HgCl_2$ and the forma-tion of HgS.

The experimental weight loss (52.63%) is significantly larger than the calculated value (38.87%). According to the results of the study,[11] the second (~263—355 °C) and third (~355—410 °C) steps can be assigned to vaporization of $HgCl_2$ and HgS. In these cases, on the contrary, the experimental weight losses (25.87 and 19.82%, respec-tively) are substantially underestimated compared to the calculated values (32.92 and 28.21%). An analysis of these data suggests that the excess weight loss in the first step (13.76%) almost completely compensates the missing weight in the second and third steps (15.44%). Therefore, taking into account the uncertainty in the separation of the steps in the TG curve, it can be concluded that $HgCl_2$ and HgS begin to vaporize already in the first step along with other volatile thermolysis products. In the gently sloping region of the TG curve (~410—600 °C), the gradual desorption of residual 1.52% weigh is observed. Upon completion of the thermolysis, a gray deposit (0.16%) was found on the crucible bottom due apparently to the partial elimination of elemental carbon.[12]

---

* The preferential formation of metal sulfides upon thermolysis of complexes with sulfur-containing ligands was substantiated in terms of thermodynamics.[30]
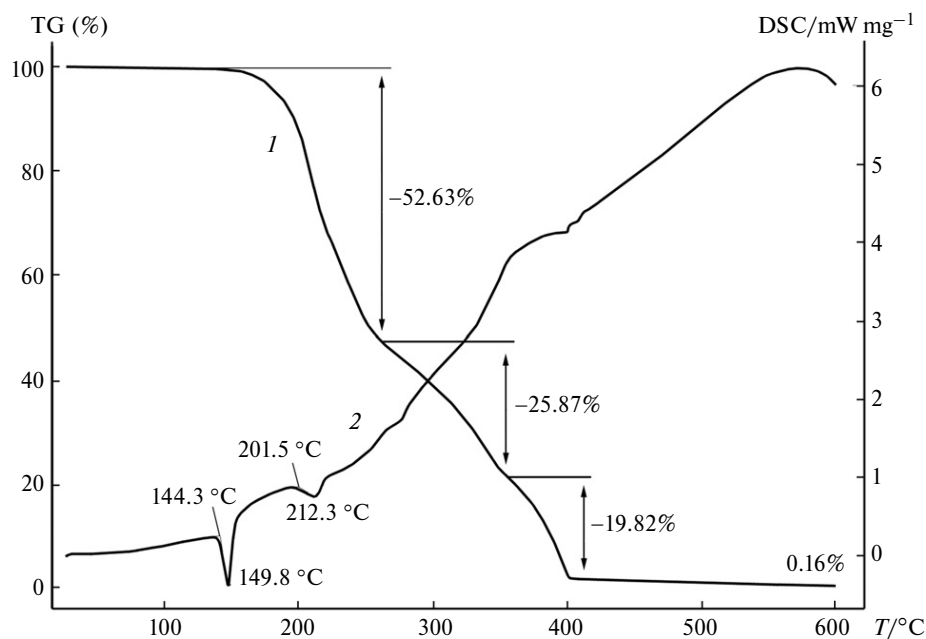

Fig. 6. TG (*1*) and DSC (*2*) curves of complex **2**.

The DSC curve of complex **2** exhibits two endothermic effects in the low-temperature region (Fig. 6, curve *2*). The first effect with an extreme at 149.8 °C is assigned to the melting of the complex (the extrapolated m.p. is 144.3 °C). In an independent experiment, the melting of the sample was determined at 144—146 °C. The second broadened endothermic effect is due to the thermolysis of complex **2**; its extreme at 212.3 °C corresponds to the maximum rate of weight loss in this TG curve region.

Experimental

Single-crystal X-ray diffraction studies of crystals of compound **1**, which were grown from a chloroform—acetone mixture (1 : 1), and crystals of **2**, which were grown from toluene, were performed on a Bruker-Nonius X8 Apex CCD diffractometer (Mo-K_α radiation, $\lambda = 0.71073$ Å, graphite monochromator) at 150(2) K. The X-ray diffraction data were collected by a standard procedure using φ- and ω-scanning of narrow frames. Absorption corrections were applied using the multi-scan method

with the SADABS program.[31] The crystal structures were solved by direct methods and refined by the full-matrix least-squares (based on F^2) with anisotropic displacement parameters. The hydrogen atoms were positioned geometrically and refined using a riding model. The structure solution and refinement were performed with the SHELXTL suite of programs.[31] The crystallographic parameters and the refinement statistics at $T = 150(2)$ K for **1** and **2** are given in Table 5.

^{13}C and ^{15}N CP-MAS NMR spectra were recorded on a Bruker Ascend Aeon 400 spectrometer operating at 100.64 and 40.55 MHz, respectively, which was equipped with a superconducting NMR magnet ($B_0 = 9.4$ T) with a closed-loop helium gas circuit through an external compressor and Fourier-transform. Cross-polarization (CP) from protons was used: the ^{1}H—^{13}C and ^{1}H—^{15}N contact time was 2.0—3.0 and 3.0—5.0 ms, respectively. The ^{13}C—^{1}H and ^{15}N—^{1}H coupling suppression was based on the decoupling effect using the radio-frequency field at the proton resonance frequency (400.21 MHz).[32] Polycrystalline samples of **1** and **2** with a weight of ~60 and ~33 mg, respectively, were placed in a 4.0 mm ZrO_2 ceramic rotor. The ^{13}C and ^{15}N NMR spectra were measured using magic-angle-spinning (MAS) of the sample at a frequency of 5000—10000 and 5000(1) Hz,

Table 5. Crystallographic parameters and the structure refinement statistics at $T = 150(2)$ K for compounds **1** and **2**

Parameter	1	2
Empirical formula	$C_{42}H_{82}Hg_4N_8O_6S_{12}$	$C_{28}H_{56}Cl_4Hg_4N_4S_8$
M_w/g mol^{-1}	1982.24	1649.41
Crystal form	Pale yellow platelet	Colorless cubic
Crystal size/mm^3	0.25×0.25×0.08	0.15×0.12×0.12
Space group	$P2_1$	$P\bar{1}$
Z	2	1
a/Å	14.5332(12)	8.6195(4)
b/Å	14.6286(10)	9.6020(4)
c/Å	15.5196(13)	14.0959(6)
α/deg	90.000	95.118(2)
β/deg	90.438(3)	90.781(2)
γ/deg	90.000	94.453(2)
V/Å^3	3299.4(4)	1158.23(9)
d_{calc}/g cm^{-3}	1.995	2.365
μ/mm^{-1}	9.703	13.832
θ-Scanning range/deg	$1.31 \leq \theta \leq 27.78$	$2.37 \leq \theta \leq 27.53$
hkl ranges	$-18 \leq h \leq 18$	$-11 \leq h \leq 11;$
	$-18 \leq k \leq 18$	$-12 \leq k \leq 8;$
	$-20 \leq l \leq 20$	$-18 \leq l \leq 18$
Number of reflections		
unique	11671	5311
with $I > 2\sigma(I)$	10905	4913
R_{int}	0.0327	0.0205
GOOF	1.078	1.043
R_1 ($F^2 > 2\sigma(F^2)$)	0.0435	0.0232
wR_2 ($F^2 > 2\sigma(F^2)$)	0.0933	0.0567
R_1 (all data)	0.0510	0.0257
wR_2 (all data)	0.0981	0.0576
Residual electron density, (ρ_{max}/ρ_{min})/ e Å^{-3}	2.573/−2.699	3.480/−2.654
CCDC*	1871184	1871185

* deposit@ccdc.cam.ac.uk or http://www.ccdc.cam.ac.uk/data_request/cif).

respectively; the number of signal transients was 3156—16924 and 3150—15360, respectively; proton $\pi/2$-pulse duration was 2.7 and 2.5 μs, respectively; pulse delays were 2.0—3.0 and 3.0—5.0 s, respectively. The isotropic chemical shifts, $\delta(^{13}C)$ and $\delta(^{15}N)$, are given relative to one of the components of the external standard — crystalline adamantane (δ 38.48 with respect to tetramethylsilane) or crystalline NH_4Cl (δ 0, −341 ppm on the absolute scale[33]), which were corrected for the magnetic field drift, the frequency equivalent of which was 0.031 and 0.011 Hz h^{-1}, respectively.

Thermal behavior of compounds **1** and **2** was studied by simultaneous thermal analysis (STA), including the simultaneous measurements of thermogravimetric (TG) and differential scanning calorimetry (DSC) curves. The measurements were performed on a NETZSCH STA 449C Jupiter instrument in closed corundum crucibles with a hole in the lid providing the vapor pressure of 1 atm during thermal decomposition of the samples. The heating rate was 5 deg min^{-1} up to 600 °C under an argon atmosphere. The sample weight was 1.278—4.381 mg; the accuracy of temperature measurements was ±0.7 °C, the accuracy of weigh measurements was ±1 · 10^{-4} mg. The TG and DSC curves were recorded using the correction file and the temperature and sensitivity calibration for the specified temperature program and heating rate. The melting points of the complexes were independently determined on a PTP(M) instrument (Khimlaborpribor).

The complexes were synthesized using the commercial reagents $Hg(NO_3)_2 \cdot H_2O$ (Fluka) and $HgCl_2$ (Fluka). Sodium dipropyldithiocarbamate was prepared by the reaction of carbon disulfide Merck with dipropylamine (Merk) in an alkaline medium[34] and was identified by ^{13}C MAS NMR (δ), $Na(S_2CNPr_2) \cdot H_2O$ (1 : 2 : 2 : 2): 208.3 ($-S_2\underline{C}N=$); 59.4, 57.9 (1 : 1, $=N\underline{C}H_2-$); 22.3, 21.5 (1 : 1, $-\underline{C}H_2-$); 12.6, 11.5 (1 : 1, $-\underline{C}H_3$)[35].

Polymeric *catena*-poly[di(μ_2-nitrato-*O*)-bis(μ_2-*N,N*-dipropyldithiocarbamato-*S,S*)-tetrakis(μ_2-*N,N*-dipropyldithiocarbamato-*S,S,S*)tetramercury(II)], ([Hg$_4${S$_2$CNPr$_2$}$_6$(NO$_3$)$_2$])$_n$ (1). A solution of $Hg(NO_3)_2 \cdot H_2O$ (0.0685 g, 0.200 mmol) in water (10 mL) was added to a solution (10 mL) containing $Na(S_2CNPr_2) \cdot H_2O$ (0.0652 g, 0.300 mmol). To prevent the hydrolysis, the solution of the salt was acidified with nitric acid to pH 2. The bulky flocculent yellowish precipitate that formed was allowed to stand for maturation for 1.5 h and then washed with distilled water, dried on a filter, and dissolved in a chloroform—acetone mixture (1 : 1). Crystals were obtained by slow evaporation of the solvent at room temperature. For the X-ray diffraction experiment, transparent pale-yellow platelet crystals of **1** were selected from a total set of the crystals.

The ^{13}C and ^{15}N MAS NMR spectroscopic characteristics (δ) of dithiocarbamate and nitrate groups in structure **1**: 202.9, 201.3, 200.1, 198.0, 196.4 (1 : 1 : 2 : 1 : 1, $-S_2\underline{C}N=$); 156.6, 155.0, 152.3, 147.9 (1 : 1 : 1 : 3, $-S_2C\underline{N}=$); 336.3 (NO_3^-); and [Hg$_2$(S$_2$CNPr$_2$)$_4$]: 204.2, 202.4 (1 : 1, $-S_2\underline{C}N=$); 144.6, 131.4 (1 : 1, $-S_2C\underline{N}=$).

Cyclic tetrakis(μ_2-*N,N*-dipropyldithiocarbamato-*S,S,S*)tetrachlorotetramercury(II), [Hg$_4$(S$_2$CNPr$_2$)$_4$Cl$_4$] (2). A solution (10 mL) containing $Na(S_2CNPr_2) \cdot H_2O$ (0.0522 g, 0.240 mmol) was added with stirring to a cooled solution of $HgCl_2$ (0.0652 g, 0.240 mmol) in water (10 mL). The greenish-yellow flocculent precipitate that formed was allowed to stand for maturation for 24 h and then washed with distilled water, dried on a filter, and dissolved in toluene on moderate heating. Transparent pale-green cubic crystals of **2** suitable for X-ray diffraction were obtained by slow evaporation of the solvent at room temperature. The yield was 84%. ^{13}C, ^{15}N MAS NMR (δ) of [Hg$_4$(S$_2$CNPr$_2$)$_4$Cl$_4$] (**2**): 198.9, 197.7 (1 : 1, $-S_2\underline{C}N=$); 60.9, 60.4, 58.3 (2 : 1 : 1, $=N\underline{C}H_2-$); 21.9, 21.2 (1 : 3, $-\underline{C}H_2-$); 13.1, 12.9, 12.0 (2 : 1 : 1, $-\underline{C}H_3$); 152.5, 152.0 (1 : 1, $-S_2C\underline{N}=$).

References

1. A. F. Wells, *Structural Inorganic Chemistry*, Clarendon Press, Oxford University Press, London, 1975, 1095 pp.
2. J. Cookson, P. D. Beer, *Dalton Trans.*, 2007, **15**, 1459.
3. M. L. Mercuri, A. Serpe, L. Marchiò, F. Artizzu, D. Espa, P. Deplano, *Inorg. Chem. Commun.*, 2014, **39**, 47.
4. S. K. Singh, R. Nandi, K. Mishra, H. K. Singh, R. K. Singh, B. Singh, *Sensor Actuat. Ser. B*, 2016, **226**, 381.
5. S. Kanchi, P. Singh, K. Bisetty, *Arab. J. Chem.*, 2014, **7**, 11.
6. N. Srinivasan, S. Thirumaran, S. Ciattini, *RSC Adv.*, 2014, **44**, 22971.
7. D. C. Onwudiwe, P. A. Ajibade, *Mat. Lett.*, 2011, **65**, 3258.
8. S. H. Dar, S. Thirumaran, S. Selvanayagam, *Polyhedron*, 2015, **96**, 16.
9. G. Gurumoorthy, S. Thirumaran, S. Ciattini, *Polyhedron*, 2016, **118**, 143.
10. O. V. Loseva, T. A. Rodina, A. I. Smolentsev, A. V. Ivanov, *Russ. J. Coord. Chem.*, 2016, **42**, 719.
11. O. V. Loseva, T. A. Rodina, A. I. Smolentsev, A. V. Ivanov, *Polyhedron*, 2017, **134**, 238.
12. O. V. Loseva, T. A. Rodina, O. N. Antzutkin, A. V. Ivanov, *Russ. J. Gen. Chem.*, 2018, **88**, 2540.
13. M. J. Cox, E. R. T. Tiekink, *Z. Kristallogr.*, 1997, **212**, 542.
14. M. J. Cox, E. R. T. Tiekink, *Z. Kristallogr.*, 1999, **214**, 571.
15. A. V. Ivanov, E. V. Korneeva, B. V. Bukvetskii, A. S. Goryan, O. N. Antzutkin, W. Forsling, *Russ. J. Coord. Chem.*, 2008, **34**, 59.
16. H. Shang, A.-X. Zheng, D. Liu, Z.-G. Ren, J.-P. Lang, *Acta Crystallogr. Sect. C*, 2011, **67**, m237.
17. R. A. Howie, E. R. T. Tiekink, J. L. Wardell, S. M. S. V. Wardell, *J. Chem. Crystallogr.*, 2009, **39**, 293.
18. M. K. Yadav, G. Rajput, A. N. Gupta, V. Kumar, M. G. B. Drew, N. Singh, *Inorg. Chim. Acta*, 2014, **421**, 210.
19. G. Rajput, M. K. Yadav, T. S. Thakur, M. G. B. Drew, N. Singh, *Polyhedron*, 2014, **69**, 225.
20. M. M. Jotani, Y. S. Tan, E. R. T. Tiekink, *Z. Kristallogr.*, 2016, **231**, 403.
21. O. V. Loseva, T. A. Rodina, A. V. Ivanov, *Russ. J. Coord. Chem.*, 2019, **45**, 22.
22. A. M. Bond, R. Colton, A. F. Hollenkamp, B. F. Hoskins, K. McGregor, *J. Am. Chem. Soc.*, 1987, **109**, 1969.
23. J. S. Casas, P. Montero-Vázquez, A. Sánchez, J. Sordo, E. M. Vázquez-López, *Polyhedron*, 1998, **17**, 2417.
24. A. V. Ivanov, A. V. Gerasimenko, O. N. Antzutkin, W. Forsling, *Inorg. Chim. Acta*, 2005, **358**, 2585.
25. D. G. Evans, J. C. A. Boeyens, *Acta Crystallogr. Sect. B*, 1988, **44**, 559.
26. A. Bondi, *J. Phys. Chem.*, 1964, **68**, 441.
27. N. W. Alcock, *Adv. Inorg. Chem. Radiochem.*, 1972, **15**, 1.

28. A. V. Ivanov, O. N. Antzutkin, *Top. Curr. Chem.*, 2005, **246**, 271.

29. M. Arshad, S.-ur-Rehman, A.H. Qureshi, K. Masud, M. Arif, A. Saeed, R. Ahmed, *Turk. J. Chem.*, 2008, **32**, 593.

30. G. A. Razuvaev, G. V. Almazov, G. A. Domrachev, M. N. Zhilina, N. V. Karyakin, *Dokl. AN SSSR* [*Dokl. Chem.*], 1987, **294**, 141 (in Russian).

31. Bruker, APEX2 (Version 1.08), SAINT (Version 7.03), SADABS (Version 2.11), SHELXTL (Version 6.12), Bruker AXS Inc., Madison, WI, USA, 2004.

32. A. Pines, M. G. Gibby, J. S. Waugh, *J. Chem. Phys.*, 1972, **56**, 1776.

33. C. I. Ratcliffe, J. A. Ripmeester, J. S. Tse, *Chem. Phys. Lett.*, 1983, **99**, 177.

34. V. M. Byr´ko, *Ditiokarbamaty* [*Dithiocarbamates*], Nauka, Moscow, 1984, 341 pp. (in Russian).

35. A. V. Ivanov, S. A. Zinkin, A. A. Konzelko, W. Forsling, *Russ. J. Inorg. Chem.*, 2004, **49**, 593.